18. Maimone A, Luigiano C, Baccarini P, et al. Preoperative diagnosis of a solid pseudopapillary tumour of the pancreas by endoscopic ultrasound fine needle biopsy: a retrospective case series. Dig Liver Dis. 2013;45:957–60.
19. Hooper K, Mukhtar F, Li S, et al. Diagnostic error assessment and associated harm of endoscopic ultrasound-guided fine-needle aspiration of neuroendocrine neoplasms of the pancreas. Cancer Cytopathol. 2013. doi:10.1002/cncy.21332).
20. Haba S, Yamao K, Bhatia V, et al. Diagnostic ability and factors affecting accuracy of endoscopic ultrasound-guided fine needle aspiration for pancreatic solid lesions: Japanese large single center experience. J Gastroenterol. 2013;48:973–81.
21. Eto K, Kawakami H, Kuwatani M, et al. Human equilibrative nucleoside transporter 1 and Notch3 can predict gemcitabine effects in patients with unresectable pancreatic cancer. Br J Cancer. 2013;108:1488–94.
22. Morin PJ, Sparks AB, Korinek V, et al. Activation of ß-catenin-Tcf signaling in colon cancer by mutations in ß-catenin or APC. Science. 1997;275:1787–90.
23. Voeller HJ, Truica CI, Gelmann EP. ß-catenin mutations in human prostate cancer. Cancer Res. 1998;58:2520–3.
24. Palacios J, Gamallo C. Mutations in the ß-catenin gene (CTNNB1) in endometrioid ovarian carcinomas. Cancer Res. 1998;58:1344–7.
25. Miyoshi Y, Iwao K, Nagasawa Y, et al. Activation of the ß-catenin gene in primary hepatocellular carcinomas by somatic alterations involving exon 3. Cancer Res. 1998;58:2524–7.
26. Liu C, Li Y, Semenov M, et al. Control of beta-catenin phosphorylation/degradation by a dual-kinase mechanism. Cell. 2002;108:837–47.
27. Wu R, Zhai Y, Fearon ER, et al. Diverse mechanisms of beta-catenin deregulation in ovarian endometrioid adenocarcinomas. Cancer Res. 2001;61:8247–55.
28. Wu G, Xu G, Schulman BA, et al. Structure of a beta-TrCP-1-Skp1-beta-catenin complex: destruction motif binding and lysine specificity of the SCF (beta-TrCP1) ubiquitin ligase. Mol Cell. 2003;11:1445–56.
29. Angulo B, Conde E, Suárez-Gauthier A, et al. A comparison of EGFR mutation testing methods in lung carcinoma: direct sequencing, real-time PCR and immunohistochemistry. PLoS One. 2012;7:e43842.
30. Gerdes B, Ramaswamy A, Simon B, et al. Analysis of beta-catenin gene mutations in pancreatic tumors. Digestion. 1999;60:544–8.
31. Jiao Y, Shi C, Edil BH, et al. DAXX/ATRX, MEN1, and mTOR pathway genes are frequently altered in pancreatic neuroendocrine tumors. Science. 2011;331:1199–203.
32. Kim JT, Li J, Jang ER, et al. Deregulation of Wnt/β-catenin signaling through genetic or epigenetic alterations in human neuroendocrine tumors. Carcinogenesis. 2013;34:953–61.
33. Rinner B, Gallè B, Trajanoski S, et al. Molecular evidence for the bi-clonal origin of neuroendocrine tumor derived metastases. BMC Genom. 2012;13:594–602.
34. Vassos N, Agaimy A, Klein P, et al. Solid-pseudopapillary neoplasm (SPN) of the pancreas: case series and literature review on an enigmatic entity. Int J Clin Exp Pathol. 2013;6:1051–9.
35. Adamthwaite JA, Verbeke CS, Stringer MD, et al. Solid pseudopapillary tumour of the pancreas: diverse presentation, outcome and histology. JOP. 2006;7:635–42.
36. Notohara K, Hamazaki S, Tsukayama C, et al. Solid pseudopapillary tumor of the pancreas, immunohistochemical localization of neuroendocrine markers and CD10. Am J Surg Pathol. 2000;24:1361–71.
37. Klöppel G, Rindi G, Anlauf M, et al. Site-specific biology and pathology of gastroenteropancreatic neuroendocrine tumors. Virchows Arch. 2007;451:S9–27.
38. Klöppel G, Couvelard A, Perren A, et al. ENETS consensus guidelines for the standards of care in neuroendocrine tumors: towards a standardized approach to the diagnosis of gastroenteropancreatic neuroendocrine tumors and their prognostic stratification. Neuroendocrinology. 2009;90:162–6.

INTERNAL MEDICINE

□ CASE REPORT □

Hepatosplenic Gamma-delta T-cell Lymphoma Associated with Epstein-Barr Virus

Seiji Tsunematsu[1], Mitsuteru Natsuizaka[1], Hiromi Fujita[2], Noriyuki Otsuka[3], Katsumi Terashita[1], Fumiyuki Sato[1], Tomoe Kobayashi[1], Masato Nakai[1], Yoko Tsukuda[1], Hiromasa Horimoto[1], Takuya Sho[1], Goki Suda[1], Mitsuru Nakanishi[1], Satoshi Hashino[1], Makoto Chuma[1] and Naoya Sakamoto[1]

Abstract

Hepatosplenic gamma-delta T-cell lymphoma (HSTCL) is a rare, aggressive subset of peripheral T-cell lymphoma. It has been reported that Epstein-Barr virus (EBV) infection can cause HSTCL; however, such cases are extremely rare, with only a few cases having been reported to date. We herein report an autopsy case of HSTCL associated with EBV infection. The presence of EBV infection was confirmed in serum EBV DNA and on *in-situ* hybridization, and cytotoxic molecules, such as granzyme B, perforin and T-cell intracytoplasmic antigen (TIA)-1, were all positive in lymphoma cells. These findings indicate that stimulation of persistent EBV infection may have caused HSTCL in this patient.

Key words: hepatosplenic gamma-delta T-cell lymphoma, Epstein-Barr virus, peripheral T-cell lymphoma, bronchiolitis obliterans organizing pneumonia, non-Hodgkin's lymphoma

(Intern Med 53: 2079-2082, 2014)
(DOI: 10.2169/internalmedicine.53.2236)

Introduction

Hepatosplenic gamma-delta T-cell lymphoma (HSTCL) is a rare extranodal T-cell non-Hodgkin's lymphoma characterized by hepatosplenomegaly without lymphadenopathy (1). Most HSTCL lesions are found in patients with autoimmune disease, chronic antigen stimulation, splenectomy and/or under immunosuppressive treatment, mostly after solid organ transplantation (2). HSTCL usually shows the phenotype of CD2+, CD3+, CD4-, CD5-, CD7+, CD8-, T cell receptor (TCR) gamma-delta+ (3, 4), while cytotoxic molecules, such as granzyme B and perforin, are usually negative in such lesions (3). Ohshima et al. reported a possible association between Epstein-Barr virus (EBV) infection and HSTCL; however, such HSTCL cases are extremely rare (5). We herein report an autopsy case of HSTCL associated with chronic EBV infection.

Case Report

A 71-year-old man was diagnosed with bronchiolitis obliterans organizing pneumonia (BOOP) five months prior to onset. He was treated with a corticosteroid, and the BOOP gradually improved. The dose of the corticosteroid was started at 30 mg/day, then tapered to 7.5 mg/day; however, it was subsequently increased again to 15 mg/day because the BOOP worsened. The corticosteroid treatment was continued at a dose of 15 mg/day, and the BOOP remained well-controlled. However, five months after the diagnosis of BOOP, the patient developed a fever and was treated with antibiotics, although the fever did not resolve. He subsequently developed severe weakness and jaundice and was referred to our department after one month. On admission, blood tests showed pancytopenia, severe liver dysfunction with hyperbilirubinemia and renal dysfunction. The levels of soluble interleukin-2 receptor (sIL-2R) and serum lactate de-

[1]Department of Gastroenterology and Hepatology, Hokkaido University, Graduate School of Medicine, Japan, [2]Department of Surgical Pathology, Hokkaido University Hospital, Japan and [3]Department of Pathology, Hokkaido University, Graduate School of Medicine, Japan
Received for publication December 2, 2013; Accepted for publication March 11, 2014
Correspondence to Dr. Makoto Chuma, mchuuma@med.hokudai.ac.jp

Table. The Patient's Laboratory Data

Parameter, units	Patient	Reference values
Cell blood counts		
WBC, ×1,000/μL	3.4	3.5-9.3
Blood smear, %		
Segmented neutrophils	82	40-70
Banded neutrophils	1	0-5
Lymphocytes	10	30-50
Monocytes	5	0-8
Atypical lymphocytes	1	0
RBC, ×10,000/μL	401	400-557
Hb, g/dL	10.8	13.4-17.6
MCV, fl	82.5	85-101
Platelets, ×1,000/μL	71	120-400
Biochemistry		
AST, U/L	315	13-33
ALT, U/L	188	8-42
CHE, U/L	192	213-501
Total bilirubin, mg/dL	3.9	0.2-1.2
Direct bilirubin, mg/dL	3.1	0-0.3
BUN, mg/dL	20	8.0-22
Cr, mg/dL	1.81	0.6-1.1
CRP, mg/L	1.8	0-0.39
Prothrombin time, %	28.3	70-130
LDH, U/L	1,622	119-229
sIL-2R, U/mL	8,125	0-459
Serological tests		
Anti-EBV IgM, M.I	<1.0	0-0.9
Anti-EBV IgG, M.I	3.5	0-0.9
EBV DNA	6.4×10^5	1×10^2
Anti-hepatitis A IgM index	0.2	0-0.7
HBsAg, IU/mL	0.01	0-0.04
Anti-HCV, S/CO	0.07	0-0.99
Anti-CMV IgM, M.I	<1.0	0-0.9
Anti-CMV IgG, G.I	50.9	0-0.9
EB V DNA (copies/mL) #	6.4×10^5	$< 1.0 \times 10^2$

#Measured in blood samples collected after death

hydrogenase (LDH) were also markedly elevated. Serological virus markers measured while the patient was alive were all negative (Table). Ultrasound and computed tomography revealed massive hepatosplenomegaly that was not observed on the computed tomography scan performed four months before onset (Fig. 1). No lymphadenopathy was detected. As a differential diagnosis, we considered hematological malignancies, including lymphoma, drug-induced liver dysfunction and viral infectious disease. A liver biopsy and bone marrow aspiration were planned to obtain a definitive diagnosis; however, the patient's clinical course was aggressive, and he died from multiple organ failure three days after admission.

An autopsy was subsequently performed, which showed the liver and spleen to be markedly enlarged, as observed earlier on ultrasound and computed tomography; their weights were 2,823 g and 814 g, respectively. No lymphadenopathy was observed. A microscopic examination revealed massive atypical lymphocyte infiltration into the liver, spleen and bone marrow. The infiltrated lymphocytes were positive for CD3 and T cell receptor (TCR)-γ and negative for CD4, CD5, CD8, CD20, CD56 and βF1 (Fig. 2, 3). The presence of atypical cells positive for TCR-γ and negative for βF1 suggested the existence of TCR gamma-delta chains. These findings indicated the tumor cells to reflect T-cell lymphoma expressing TCR gamma-delta chains. Interestingly, *in-situ* hybridization for EBV and cytotoxic molecules, including granzyme B, perforin and T-cell intracytoplasmic antigen (TIA)-1 were all positive in the lymphoma cells (Fig. 2), indicating a persistent infection of EBV with a cytotoxic reaction. The phenotypes of the lymphoma cells in the liver, spleen and bone marrow were exactly the same. Accordingly, we later measured the EBV DNA titer in the patient's stored serum, which revealed a high level of EBV DNA (Table). The patient's condition was diagnosed as HSTCL associated with EBV infection.

Discussion

HSTCL is a rare subset of peripheral T-cell lymphoma that accounts for less than 1% of all non-Hodgkin's lymphomas (6). HSTCL has a peak incidence in adolescents and young adults. Patients with HSTCL commonly show hepatosplenomegaly in the absence of lymphadenopathy (1). Pancytopenia is also a common feature of HSTCL due to bone marrow involvement (7). The clinical course of HSTCL is aggressive, with a reported median survival time of eight months (3). No effective combination chemotherapy has been documented to date, and the only curative treatment is allogeneic stem cell transplantation (8). The patient in the present case report was relatively old; however, he exhibited the typical symptoms of HTSCL, including hepatosplenomegaly, thrombocytopenia, fever and weakness, and his clinical course was extremely aggressive.

HSTCL usually carries the phenotype of CD2+, CD3+, CD4-, CD5-, CD7+, CD8-, TCR gamma-delta+, and it is assumed that HTSCL may originate from gamma-delta TCR-expressing T-cells. Such T-cells demonstrate preferential homing to the sinusoidal areas of the liver, red pulp of the spleen and epithelial layer of the intestinal mucosa (9). The lymphoma cells of HTSCL have similar characteristics and infiltrate into the sinusoidal areas of the liver, bone marrow and red pulp of the spleen without lymph node involvement. Most HSTCL cases express only TIA-1, not other cytotoxic molecules, such as granzyme B and perforin (10). In contrast, non-hepatosplenic gamma-delta T-cell lymphomas, including nasal, cutaneous and intestinal gamma-delta T-cell lymphomas, often express all of cytotoxic molecules, and, interestingly, some are associated with EBV infection (11). Although various lymphomas, including nasal natural killer (NK)/T-cell lymphomas, are caused by EBV infection (12), only two cases of HTSCL associated with EBV have been reported thus far (5). In both cases, all cytotoxic molecules (TIA-1, granzyme B and perforin) were expressed, and the patients died within one month. In the present case, we confirmed EBV infection on *in-situ* hybridization of the EBV region, and almost all of the lymphoma cells were positive. Furthermore, the lymphoma cells expressed all of the cytotoxic molecules, including TIA-1 and granzyme B, and the

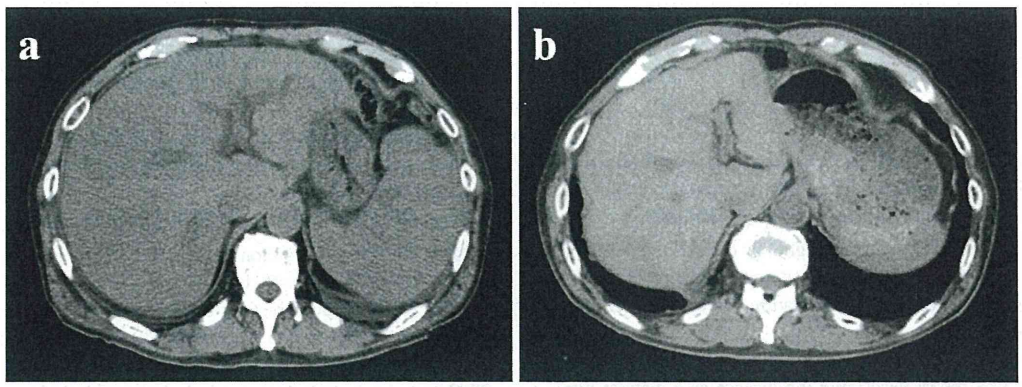

Figure 1. **Computed tomography (CT) of the abdomen, transverse scan. (a) CT scan obtained at time of admission. (b) CT scan obtained five months before admission. The liver and spleen were enlarged on the last CT scan compared to that observed on the previous CT scan.**

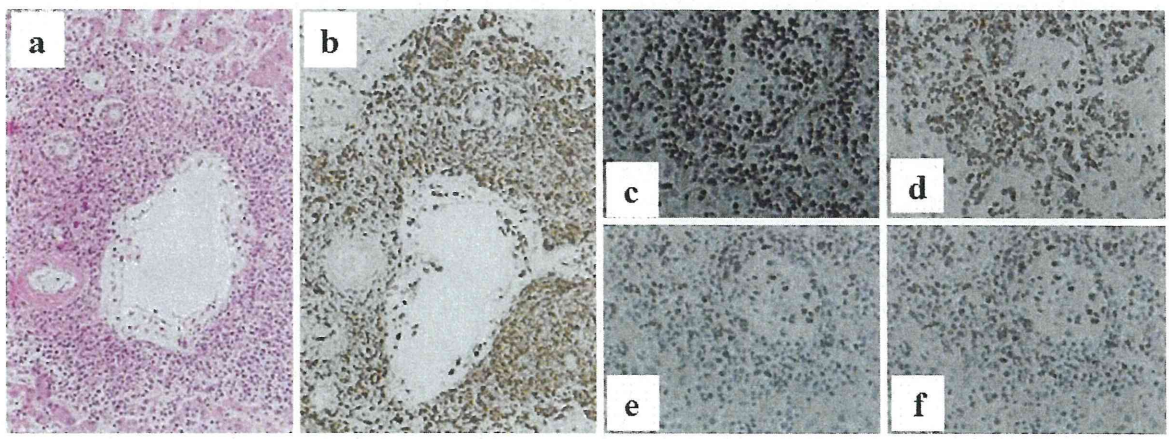

Figure 2. **Histological features and immunohistochemical staining as well as *in-situ* hybridization with EBER-1 antisense oligonucleotides. The histological features of the liver showed lymphoma cell infiltration in the hepatic sinusoids with mild involvement of the portal areas (a). The atypical cells were positive for CD3 and (b) *in-situ* hybridization with EBER-1 antisense oligonucleotide (c), granzyme B (d), TIA-1 (e) and perforin (f). (Original magnification: A, B ×20; C, D, E ×40)**

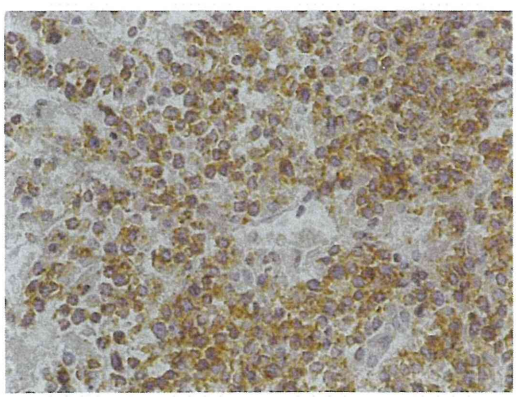

Figure 3. **Immunohistochemical staining for TCR-γ. The atypical cells were positive for TCR-γ. (Original magnification: ×40)**

patient's clinical course was extremely aggressive. It is possible that EBV infection may either cause or accelerate HSTCL and activate cytotoxic molecules, leading to an extremely poor prognosis.

In conclusion, we herein reported an extremely rare case of HSTCL associated with EBV infection. The present case implies a possible association between HSTCL and EBV; however, the detailed mechanism by which EBV affects the onset of HSTCL remains to be elucidated. Further studies and the accumulation of cases of EBV-associated HSTCL are necessary.

The authors state that they have no Conflict of Interest (COI).

Acknowledgement

We thank Yoshihiro Matsuno (Department of Surgical Pathology, Hokkaido University Hospital, Japan) and Ohshima Kouichi

(Department of Pathology, School of Medicine, Kurume University, Japan).

References

1. Belhadj K, Reyes F, Farcet JP, et al. Hepatosplenicγδ T-cell lymphoma is a rare clinicopathologic entity with poor outcome:report on a series of 21 patients. Blood **102**: 4261-4269, 2003.
2. Roelandt PR, Maertens J, Vandenberghe P, et al. Hepatosplenic gammadelta T-cell lymphoma after liver transplantation: report of the first 2 cases and review of the literature. Liver Transplant **15**: 686-692, 2009.
3. Weidmann E. Hepatosplenic T cell lymphoma. A review on 45 cases since the first report describing the disease as a distinct lymphoma entity in 1990. Leukemia **14**: 991-997, 2000.
4. Gaulard P, Belhadj K, Reyes F. Gammadelta T-cell lymphomas. Semin Hematol **40**: 233-243, 2003.
5. Ohshima K, Haraoka S, Harada N, et al. Hepatosplenic γδ T-cell lymphoma: relation to Epstein-Barr virus and activated cytotoxic molecules. Histopathology **36**: 127-135, 2000.
6. Cooke CB, Krenacs L, Stetler-Stevenson M, et al. Hepatosplenic T-cell lymphoma: a distinct clinicopathologic entity of cytotoxic gamma delta T-cell origin. Blood **88**: 4265-4274, 1996.
7. Belhadj K, Reyes F, Farcet JP, et al. Hepatosplenic gammadelta T-cell lymphoma is a rare clinicopathologic entity with poor outcome: report on a series of 21 patients. Blood **102**: 4261-4269, 2003.
8. Falchook GS, Vega F, Dang NH, et al. Hepatosplenic gamma-delta Tcell lymphoma: clinicopathological features and treatment. Ann Oncol **20**: 1080-1085, 2009.
9. Bucy RP, Chen CL, Cooper MD. Tissue localization and CD8 accessory molecule expression of T gamma delta cells in humans. J Immunol **142**: 3045-3049, 1989.
10. Belhadj K, Reyes F, Farcet JP, et al. Hepatosplenic gammadelta T-cell lymphoma is a rare clinicopathologic entity with poor outcome: report on a series of 21 patients. Blood **102**: 4261-4269, 2003.
11. Arnulf B, Copie-Bergman C, Delfau-Larue MH, et al. Nonhepatosplenic gamma delta T-cell lymphoma:a subset of cytotoxic lymphomas with mucosal or skin localization. Blood **91**: 1723-1731, 1998.
12. Harabushi Y, Imai S, Wakashima J, et al. Nasal T-cell lymphoma causally associated with Epstein-Barr virus. Cancer **77**: 2137-2149, 1996.

Hepatology Research

Hepatology Research 2014 doi: 10.1111/hepr.12421

Original Article

Serum granulysin levels as a predictor of serious telaprevir-induced dermatological reactions

Goki Suda,[1] Yoshiya Yamamoto,[2] Astushi Nagasaka,[3] Ken Furuya,[4] Mineo Kudo,[5] Yoshimichi Chuganji,[6] Yoko Tsukuda,[1] Seiji Tsunematsu,[1] Fumiyuki Sato,[1] Katsumi Terasita,[1] Masato Nakai,[1] Hiromasa Horimoto,[1] Takuya Sho,[1] Mitsuteru Natsuizaka,[1] Kouji Ogawa,[1] Shunsuke Ohnishi,[1] Makoto Chuma,[1] Yasuyuki Fujita,[7] Riichiro Abe,[7] Miki Taniguchi,[8] Mina Nakagawa,[8] Yasuhiro Asahina[8] and Naoya Sakamoto[1] for the NORTE Study Group

[1]*Department of Gastroenterology and Hepatology, Graduate School of Medicine, Hokkaido University,* [2]*Hakodate City Hospital,* [3]*Sapporo City General Hospital,* [4]*Hokkaido Social Insurance Hospital,* [5]*Sapporo Hokuyu Hospital,* [7]*Department of Dermatology, Hokkaido University Graduate School of Medicine, Hokkaido,* [6]*Tokyo Metropolitan Bokuto Hospital, and* [8]*Department of Gastroenterology and Hepatology, Tokyo Medical and Dental University, Tokyo, Japan*

Aim: Telaprevir-based therapy for chronic hepatitis C patients is effective; however, the high prevalence of dermatological reactions is an outstanding issue. The mechanism and characteristics of such adverse reactions are unclear; moreover, predictive factors remain unknown. Granulysin was recently reported to be upregulated in the blisters of patients with Stevens–Johnson syndrome (SJS). Therefore, we investigated the risk factors for severe telaprevir-induced dermatological reactions as well as the association between serum granulysin levels and the severity of such reactions.

Methods: A total of 89 patients who received telaprevir-based therapy and had complete clinical information were analyzed. We analyzed the associations between dermatological reactions and clinical factors. Next, we investigated the time-dependent changes in serum granulysin levels in five and 14 patients with grade 3 and non-grade 3 dermatological reactions, respectively.

Results: Of the 89 patients, 57 patients had dermatological reactions, including nine patients with grade 3. Univariate analysis revealed that grade 3 dermatological reactions were significantly associated with male sex. Moreover, serum granulysin levels were significantly associated with the severity of dermatological reactions. Three patients with grade 3 dermatological reaction had severe systemic manifestations including SJS, drug-induced hypersensitivity syndrome, and systemic lymphoid swelling and high-grade fever; all were hospitalized. Importantly, among the three patients, two patients' serum granulysin levels exceeded 8 ng/mL at onset and symptoms deteriorated within 6 days.

Conclusion: Male patients are at high risk for severe telaprevir-induced dermatological reactions. Moreover, serum granulysin levels are significantly associated with the severity of dermatological reactions and may be a predictive factor in patients treated with telaprevir-based therapy.

Key words: drug-induced hypersensitivity syndrome, granulysin, hepatitis C virus, telaprevir, toxic epidermal necrolysis

INTRODUCTION

HEPATITIS C IS a major pathogen causing liver cirrhosis and hepatocellular carcinoma worldwide. Until recently, standard therapies for chronic hepatitis C virus (HCV) genotype 1 infection were based on the combination of pegylated interferon (PEG IFN) and ribavirin (RBV); these combination therapies yield a sustained virological response (SVR) rate of approximately 50%.[1] Several classes of novel direct-acting antivirals

Correspondence: Dr Goki Suda, Department of Gastroenterology and Hepatology/Graduate School of Medicine, Hokkaido University, North 15, West 7, Kita-ku, Sapporo, Hokkaido 060-8638, Japan. Email: gsudgast@pop.med.hokudai.ac.jp

Conflict of interest: The authors declare that they have nothing to disclose regarding funding from the industry or conflicts of interest with respect to the manuscript.

Received 9 June 2014; revision 27 August 2014; accepted 4 September 2014.

(DAA) were recently developed and tested in clinical trials. Two first-generation HCV NS3/4A protease inhibitors, boceprevir[2,3] and telaprevir,[4–6] have been approved for the treatment of genotype 1 HCV infection. The inclusion of these agents in HCV treatment regimens has led to large improvements in treatment success rates.

Telaprevir, the first DAA, is administrated in combination with PEG IFN and RBV for 24 weeks, resulting in SVR rates up to 70–80%.[4,6–8] Although the telaprevir combination regimen is highly effective, the high frequency and severity of adverse events are outstanding issues limiting its use. Dermatological reactions are particularly prevalent, developing in 56–84.6% of patients treated with telaprevir, PEG IFN and RBV combination therapy.[9,10] Moreover, the prevalence of severe dermatological reactions including Stevens–Johnson syndrome/toxic epidermal necrolysis (SJS/TEN) and drug-induced hypersensitivity syndrome (DIHS) are substantially higher in patients treated with telaprevir-based therapy than PEG IFN and RBV combination therapy.[8,10] McHutchison *et al.* reported that 7% of patients treated with telaprevir, PEG IFN and RBV combination therapy discontinue therapy because of rash or pruritus in contrast to only 1% of patients treated with PEG IFN and RBV.[8] In some patients, serious skin reactions persist even after stopping all drugs.[10] However, the pathogenesis and clinical predictors of these adverse reactions are poorly understood.

Granulysin is a 15-kDa cationic cytolytic protein released by cytotoxic T lymphocytes and natural killer cells that induces apoptosis in target cells and has antimicrobial activities.[11] Serum levels of granulysin are elevated in primary virus infections including Epstein–Barr virus and parvovirus B19.[12] It was recently reported that serum granulysin levels are significantly elevated in patients with several types of severe dermatological lesions including SJS/TEN, which is the characteristic serious adverse event in telaprevir-containing regimens.[13,14]

Accordingly, the present study determined the risk factors for severe dermatological reactions in patients receiving telaprevir, PEG IFN and RBV combination therapy as well as the association between serum levels of granulysin and severe dermatological reactions.

METHODS

Patients and methods

IN THIS RETROSPECTIVE case–control study, at Hokkaido University Hospital and associated hospitals in the NORTE Study Group, between December 2011 and November 2013, a total of 123 patients positive for HCV genotype 1 with high serum HCV RNA titer (>5 log IU/mL) received PEG IFN, RBV and telaprevir combination therapy. Patients were excluded if they required hemodialysis or had a positive test result for serum hepatitis B surface antigen, co-infection with other HCV genotypes or HIV, evidence of autoimmune hepatitis or alcoholic hepatitis, or malignancy. Serum granulysin levels were analyzed in five healthy volunteers with no HCV, HIV or hepatitis B virus infection or any inflammatory diseases.

Written informed consent according to the process approved by the hospital's ethics committee was obtained from each patient. The study protocol conformed to the ethical guidelines of the Declaration of Helsinki and was approved by the ethics committee of each participating hospital.

Study design and treatment regimen

Telaprevir 500 or 750 mg was typically administrated every 8 h after meals for 12 weeks. PEG IFN-α-2b (Peg-Intron; MSD, Tokyo, Japan) 1.5 IU/kg was administrated s.c. once per week for 24 weeks. RBV (Rebetol; MSD) was administrated for 24 weeks in two divided daily doses according to bodyweight: 600, 800 and 1000 mg for patients with bodyweights of less than 60, 60–80 and more than 80 kg, respectively. The doses of PEG IFN-α-2b, RBV and telaprevir were reduced at the attending physician's discretion on the basis of hemoglobin levels, decreased white blood cell or platelet counts, or adverse events.

During treatment, patients were assessed as outpatients at weeks 1, 2, 4, 6 and 8, and then every 4 weeks thereafter for the duration of treatment. Physical examinations and blood tests were performed at all time points.

Outcomes

The primary end-point was SVR, which was defined as undetectable serum HCV RNA at 24 weeks after the end of treatment. The secondary end-points were end-of-treatment virological responses (HCV RNA undetectable in serum) and rapid virological response (RVR), which was defined as undetectable serum HCV RNA at 4 weeks after the start of treatment. Dermatological reactions were classified according to severity in the same manner as in phase III trials in Japan.[10]

Serum granulysin measurement

To evaluate serum granulysin levels in chronic hepatitis C, we first measured serum granulysin levels in five

healthy volunteers and compared them with those of 20 chronic hepatitis C patients before treatment. Serum granulysin levels were measured at the onset of dermatological reactions (within 3 days of onset); if the symptoms worsened, the time when worsening occurred was adopted. Meanwhile, in patients with no dermatological reactions, the highest serum granulysin level during treatment was adopted.

Serum granulysin levels were measured by a sandwich enzyme-linked immunosorbent assay as described previously.[12,14,15] Briefly, plates coated with 5 mg/mL mouse antibody against human granulysin, RB1 antibody, were washed with phosphate-buffered saline containing 0.1% Tween-20. Next, they were blocked with 10% fetal bovine serum in washing buffer at room temperature for 2 h. The samples and standards (Recombinant Granulysin; R&D Systems, Minneapolis, MN, USA) were incubated for 2 h at room temperature. Next, they were reacted with 0.1 mg/mL biotinylated mouse antibody against human granulysin, RC8 antibody. The plates were subsequently treated with horseradish peroxidase-conjugated streptavidin (Roche Diagnostics, Basel, Switzerland). The plates were then incubated with tetramethyl-benzidine substrate (Sigma, St Louis, MO, USA), and 1 M sulfuric acid was then added. The optical density was measured at 450 nm using a microplate reader.

Diagnosis of dermatological reactions

Dermatological reactions were investigated throughout the 24-week administration period in the telaprevir-based combination therapy. Dermatological reactions were classified according to severity as follows. Grade 1 was defined as involvement of less than 50% of the body surface and no evidence of systemic symptoms. Grade 2 was defined as involvement of less than 50% of the body surface but with multiple or diffuse lesions or rashes with characteristic mild systemic symptoms or mucous membrane involvement with no ulceration/erosion. Grade 3 was defined as a generalized rash involving 50% or more of the body surface or a rash with any new significant systemic symptoms and considered to be related to the onset and/or progression of the rash. Life-threatening reactions included SJS, TEN, drug rash with eosinophilia and systemic symptoms (DRESS)/DIHS, erythema multiforme and other life-threatening symptoms, or patients presenting with features of serious disease.

When adverse skin reactions were detected, the attending physician classified the degree of severity and referred the patients to a dermatologist as needed. In principal, when grade 3 dermatological reactions occurred, the attending physician referred the patient to a dermatologist and discontinued telaprevir. When severe dermatological reactions including SJS/TEN and DRESS/DIHS were suspected, all drugs were discontinued immediately. SJS/TEN and DIHS were diagnosed by skin biopsy and according to disease criteria, respectively.

Statistical analysis

Categorical and continuous variables were analyzed by the χ^2-test and the unpaired Mann–Whitney *U*-test, respectively. All *P*-values were two-tailed, and the level of significance was set at $P < 0.05$. Multivariate logistic regression analysis with stepwise forward selection included variables showing $P < 0.05$ in univariate analyses.

The association between dermatological reactions and serum granulysin levels were evaluated by one-way ANOVA followed by Tukey's honestly significant difference test. All statistical analyses were performed using SPSS version 21.0 (IBM Japan, Tokyo, Japan).

RESULTS

Patients

WE INCLUDED 123 chronic hepatitis C patients who received telaprevir-based triple therapy. Of these, 89 patients who had proper information of dermatological adverse events were included. The baseline characteristics of patients are shown in Table 1.

Of these 89 patients, time-dependent changes of serum granulysin concentrations were measured in 20 who had had conserved serum, at least, at the pretreatment point, 1 and 2 weeks after commencement of therapy, 1 and 2 months after commencement of therapy, the onset point of dermatological adverse reaction and the worsening point if symptoms became worse.

Among the 89 patients, 64% (57/89) developed dermatological reactions, including nine with grade 3 reactions (Table 2). The characteristics of dermatological reactions by grade are shown in Table 2. Non-grade 3 dermatological reactions tended to occur early during treatment compared to grade 3 dermatological reactions.

Association between dermatological reactions and treatment outcomes

First, we determined whether dermatological reactions were associated with final treatment outcomes.

Table 1 Baseline characteristics of the participating patients

Total number	89
HCV genotype 1b (1b/others)	89/0
Age (years)†	60.0 (19–73)
Sex (male/female)	48/41
Bodyweight (kg)†	63.0 (32–97)
Baseline white blood cell count (/μL)†	4800 (1500–9800)
Baseline hemoglobin level (g/dL)†	13.5 (9.9–16.7)
Baseline platelet count ($\times 10^3$)†	15.9 (6.6–86)
Baseline ALT level (IU/L)†	40 (15–300)
Baseline HCV RNA level ($\log^{10}$ IU/mL)†	6.5 (3.2–7.6)
Initial telaprevir dose (1500/2250 mg)	20/89
Initial PEG IFN dose (1.5/<1.5 μg/kg)	775/14
Initial RBV dose (mg/kg)†	9.8 (2.2–15.5)
IL28B gene (rs8099917) (TT/non-TT/ ND)	51/22/16
HCV 70 core mutation (wild/ mutant/ND)	43/24/22
Previous treatment (naïve/relapse/NVR)	40/38/11

†Data are shown as median (range) values.
ALT, alanine transaminase; HCV, hepatitis C virus; IL28B, interleukin 28B; ND, not done; PEG IFN, pegylated interferon; RBV, ribavirin.

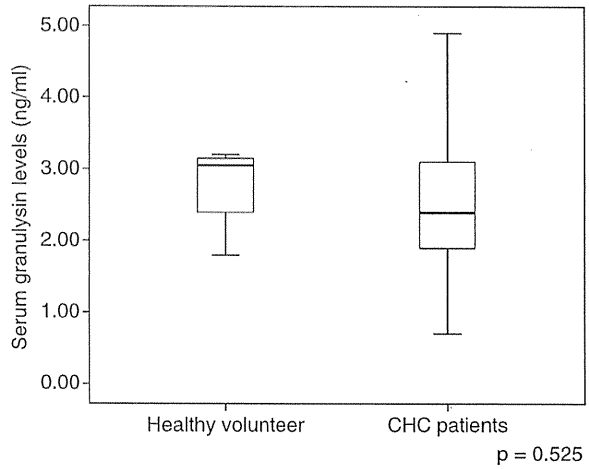

Figure 1 Serum granulysin levels of healthy volunteers and chronic hepatitis C patients. Serum granulysin levels were compared between five healthy volunteers and untreated 20 chronic hepatitis C patients. $P < 0.05$, Mann–Whitney *U*-test.

Univariate analyses identified baseline white blood cell and platelet counts, RVR, and non-grade 3 dermatological reactions significantly associated with SVR (Table 3). Among the nine patients with grade 3 dermatological reactions, three discontinued all treatment and six discontinued telaprevir administration; SVR was achieved in zero of the three (0%) and two of the six (33%), respectively.

Multivariate analysis showed that RVR and non-grade 3 dermatological reactions were significantly associated with SVR (Table 3).

Analysis of risk factors for telaprevir-induced dermatological reactions

Next, we analyzed the association between severe (i.e. grade 3) dermatological reactions and clinical parameters (Table 4). Univariate analysis showed that only sex was significantly associated with the grade 3 dermatological reactions ($P = 0.03$).

Serum granulysin levels in healthy subjects and chronic hepatitis C patients

As shown in Figure 1, serum granulysin levels did not differ significantly between healthy volunteers and chronic hepatitis C patients. Next, we evaluated the association between the severity of dermatological reactions and serum peak granulysin levels in 20 patients including five, four, five and six with grades 1, 2 and 3, and no dermatological events, respectively. One-way ANOVA showed that serum granulysin level was significantly associated with the severity of dermatological reactions ($P = 0.036$); in addition, Tukey's honestly significant difference test revealed that the serum

Table 2 Characteristics of the patients with each dermatological adverse event grade

	n	Age†	Sex (male/female)	Initial telaprevir dose (2250/1500)	Onset of DAR (days)
No DAR	32	61 (28–72)	15/17	26/6	
Grade 1	32	58 (19–73)	15/17	24/8	7 (3–50)
Grade 2	16	61 (44–73)	10/6	12/4	3.5 (1–56)
Grade 3	9	61 (48–65)	8/1	8/1	22 (1–60)

†Data are shown as median range) values.
DAR, dermatological adverse reaction

Table 3 Comparison of the clinical and laboratory characteristics of the patients with HCV infection based on therapeutic response

All patients	SVR	Non-SVR	Univariate analysis	Multivariate analysis		
$n = 89$	$n = 68$	$n = 21$	P	OR	95% CI	P
Age (years)†	60 (19–73)	62 (28–73)	0.402			
Sex (male/female)	37/31	11/10	0.870			
Bodyweight (kg)†	62 (39–97)	64 (32–87)	0.761			
Baseline white blood cells (/μL)†	5135 (1500–9800)	4200 (2490–7200)	0.048	0.492	(0.121–1.993)	0.320
Baseline hemoglobin level (g/dL)†	13.5 (10.5–16.7)	12.1 (9.9–15.4)	0.862			
Baseline platelet count ($\times 10^3$)†	16.7 (6.6–31.5)	12.8 (7.2–86)	0.025	0.388	(0.093–1.614)	0.193
Baseline ALT level (IU/L)†	37 (15–300)	53 (23–159)	0.070			
Baseline HCV RNA level ($\log^{10}$ IU/mL)†	6.7 (3.2–7.6)	6.4 (5.7–7.3)	0.812			
Baseline Cr level (mg/dL)	0.7 (0.5–1.3)	0.7 (0.5–0.9)	0.433			
Initial telaprevir dose (1500/2250 mg)	52/16	17/4	0.460			
Initial PEG IFN dose (1.5/<1.5 μg/kg)	58/10	17/4	0.430			
Initial RBV dose (mg/kg)†	9.9 (2.2–15.5)	9.5 (4.4–12.5)	0.546			
IL28B gene (rs8099917) (TT/non-TT/ND)	43/15/10	8/7/6	0.107			
Core 70 a.a. mutation (wild/mutant/ND)	36/16/16	7/8/6	0.108			
Previous treatment (naive/relapse/NVR)	34/28/6	6/10/5	0.095			
Rapid virological response (+/−)	60/8	10/11	<0.001	10.89	(2.838–41.83)	0.001
Grade 3 DAR (−/+)	66/2	14/7	<0.001	27.44	(3.718–202.5)	0.001

†Data are shown as median (range) values.
a.a., amino acid; ALT, alanine transaminase; CI, confidence interval; Cr, creatinine; DAR, dermatological adverse reaction; HCV, hepatitis C virus; IL28B, interleukin 28B; ND, not done; NVR, non-virological response; OR, odds ratio; PEG IFN, pegylated interferon; SVR, sustained virological response; RBV, ribavirin.

granulysin levels of patients with grade 3 dermatological reactions were significantly higher than those of patients with grade 1 or no dermatological reactions (both $P < 0.05$, Fig. 2).

Time-dependent changes in serum granulysin levels

We investigated the time-dependent changes in serum granulysin levels in five and 15 patients with grade 3 and non-grade 3 dermatological reactions, respectively (Fig. 3). Serum granulysin levels of patients with non-grade 3 dermatological reactions never exceeded 10 ng/ml. Of the five patients with grade 3 reactions, three had severe systemic manifestations that necessitated hospital admission: one each had SJS, DIHS, and systemic lymphoid swelling and high fever (>39 °C). All patients with grade 3 dermatological reactions with systemic manifestations had peak serum granulysin levels exceeding 10 ng/mL; importantly, the serum granulysin levels of two patients already exceeding 8 ng/mL at the onset of the reactions worsened within 6 days.

DISCUSSION

THE PRESENT STUDY demonstrates a significant association between telaprevir-induced dermatological reactions and elevated serum granulysin levels for the first time. Moreover, serum granulysin levels were significantly associated with the severity of dermatological reactions. Thus, the results indicate that serum granulysin level seems to be a useful predictor of telaprevir-induced dermatological reactions. Because the emergence of grade 3 dermatological reactions was significantly associated with non-SVR (Table 3), probably associated with high rate of treatment discontinuation, it is important to predict dermatological events in the early stage to achieve good treatment outcomes.

Table 4 Comparison of the clinical and laboratory characteristics of the patients based on the presence or absence of at least a grade 3 dermatological adverse event

All patients $n = 89$	Non-grade 3 $n = 80$	Grade ≥3 $n = 9$	Univariate analysis P
Age (years)†	60 (19–73)	61 (48–65)	0.453
Sex (male/female)	40/40	8/1	0.027
Bodyweight (kg)†	62 (32–97)	64 (51–87)	0.593
Baseline white blood cell count (/μL)†	4900 (1500–9800)	4700 (3000–7000)	0.876
Baseline hemoglobin level (g/dL)†	13.5 (9.9–16.7)	14.4 (12.1–15.4)	0.196
Baseline platelet count ($\times 10^3$)†	16.0 (6.6–86.0)	13.5 (10.4–22.5)	0.605
Baseline ALT level (IU/L)†	40(15–300)	37 (23–87)	0.765
Baseline Cr level (mg/dL)	0.7 (0.5–1.3)	0.8 (0.6–0.9)	0.123
Baseline HCV RNA level ($\log^{10}$ IU/mL)†	6.6 (3.2–7.6)	6.4 (5.7–7.1)	0.465
Initial telaprevir dose (1500/2250 mg)	62/18	7/2	0.675
Initial telaprevir/bodyweight (mg/kg)	33.7 (20–71.4)	30.0 (23.6–44.1)	0.563
Initial PEG IFN dose (1.5/<1.5 μg/kg)	66/14	9/0	0.198
Initial RBV dose (mg/kg)†	9.7 (2.2–15.5)	10.7 (7.7–12.9)	0.161
IL28B gene (rs8099917) (TT/non-TT/ND)	47/19/14	4/3/2	0.353
Core 70 a.a. mutation (wild/mutant/ND)	38/22/20	5/2/2	0.511
Previous treatment (naïve/relapse/NVR)	35/36/9	5/2/2	0.972
Onset of dermatological AE (days)	5 (1–75)	22 (1–60)	0.352

†Data are shown as median (range) values.
a.a., amino acid; AE, adverse event; ALT, alanine transaminase; Cr, creatinine; HCV, hepatitis C virus; IL28B, interleukin 28B; NVR, non-virological response; PEG IFN, pegylated interferon; RBV, ribavirin.

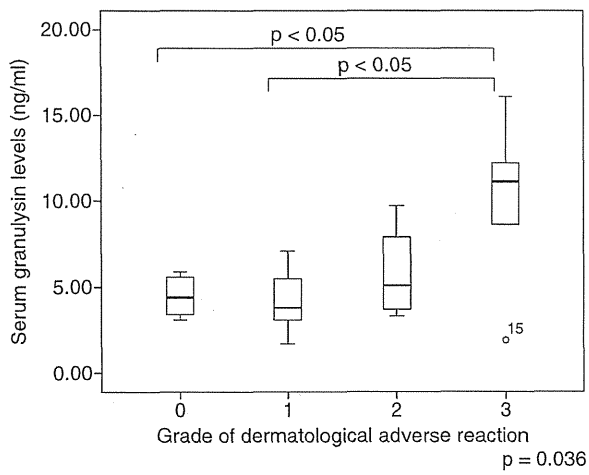

Figure 2 Association between dermatological adverse reaction severity and serum granulysin level. Serum granulysin levels were measured at the onset of dermatological reactions (i.e. within 3 days of onset); if the symptoms worsened, the time of worsening was adopted. In patients with no dermatological events, the highest serum granulysin level during treatment was adopted. $P < 0.05$, one-way ANOVA.

Recent genome-wide association studies have identified that genetic polymorphisms around the IL28B gene locus significantly associated with the outcome of PEG IFN and RBV combination therapy in HCV patients. Thus, PEG IFN and RBV combination therapy is ineffective in a subset of HCV-infected patients who have IL28B TG or GG genotypes, limiting the use of this therapy.[16] Therefore, novel drugs with different antiviral mechanisms were required. Accordingly, DAA were developed; they are mainly classified as NS3/4A protease inhibitors, or NS5B or NS5A inhibitors.[17] The NS3/4A serine protease inhibitor telaprevir, in combination with PEG IFN and RBV, has demonstrated the most promising results.[6–8] However, adverse events, especially severe dermatological reactions, develop more frequently in patients treated with telaprevir than those treated with only PEG IFN and RBV.

Little is known about the mechanisms of telaprevir-induced dermatological reactions. Reactions develop in patients treated with PEG IFN and RBV combination therapy[18,19] as well as telaprevir monotherapy.[20,21] It should be noted that the dermatological reactions in telaprevir monotherapy or PEG IFN and RBV therapy alone are generally mild.[7,8,20] However, dermatological

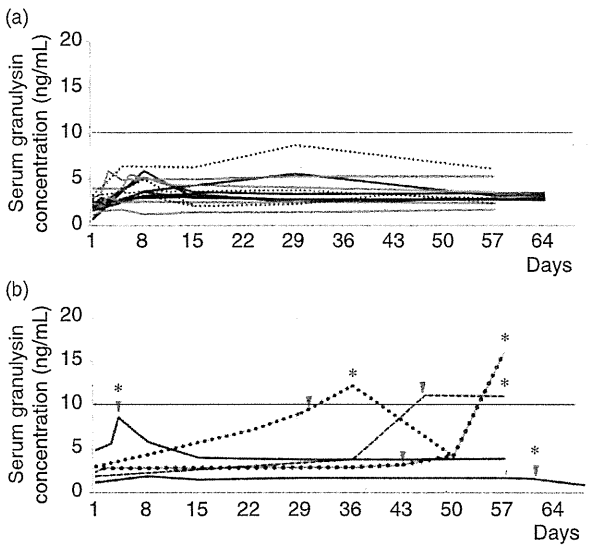

Figure 3 Association between time-dependent changes in serum granulysin levels and severe telaprevir-induced dermatological adverse reactions. (a) Time-dependent changes in serum granulysin levels patients with non-grade 3 dermatological reactions (three, five and six with grade 2, grade 1 and no reactions, respectively). The dashed line, gray line and black line indicate grade 2, grade 1 and no reaction, respectively. (b) Time-dependent changes in serum granulysin levels of five patients with grade 3 dermatological events. The dashed line indicates patients with severe systemic manifestations. Arrowheads indicate the onset of dermatological events and asterisks indicate the onset of grade 3 dermatological events.

reactions in telaprevir and PEG IFN/RBV combination therapy may be severe, indicating a synergistic effect. Severe dermatological events including SJS/TEN and DIHS have been reported in telaprevir-based triple therapy; these are life-threatening, and fatal cases have been reported.

The onset of grade 3 dermatological reactions tended to be later than non-grade 3 reactions, the same as in the study of Torii *et al.*[10] Taken together with the finding that male sex is a clinical risk factor, the results indicate that late-onset dermatological reactions in male patients treated with telaprevir-based triple therapy require more attention.

Roujeau *et al.* analyzed the risk factors for telaprevir-induced eczematous dermatitis and report that the incidence of telaprevir-related dermatitis was significantly higher age of more than 45 years, body mass index of less than 30 (kg/m^2), Caucasian ethnicity and treatment-naïve status.[9] While they analyzed the risk factors for telaprevir-induced eczematous dermatitis, the present study focused on the risk factors for severe telaprevir-induced dermatological reactions, because such reactions can affect treatment outcome (Table 2) and can be fatal. As mentioned above, male sex was significantly associated with grade 3 dermatological reactions. Sex is reported to be associated with the prevalence of some kinds of severe drug-induced dermatological events, although the underlying mechanism remains unknown.[22]

Fujita *et al.* report that serum granulysin levels are significantly elevated in SJS/TEN patients and thus may be a good predictive factor.[14] Therefore, we hypothesized that in telaprevir-based triple therapy for chronic hepatitis C patients, serum granulysin levels are associated with the severity of dermatological reactions and may thus be a predictive biomarker. However, Ogawa *et al.* report that serum granulysin levels also increase as a result of primary virus infections such as Epstein–Barr virus or parvovirus B19.[12] Thus, it remains unclear whether and how chronic viral infections, especially HCV, affect serum granulysin levels. In the present study, we compared serum granulysin levels between healthy volunteers and chronic hepatitis C patients; the results show that chronic HCV infection was not associated with serum granulysin levels (Fig. 1).

Chung *et al.* have reported that granulysin is the most highly expressed cytotoxic molecule in blisters of SJS/TEN and that massive keratinocyte death was induced by granulysin.[11] Fujita *et al.* reported that serum granulysin levels increased in the early stage of SJS/TEN caused by drugs including carbamazepine, imatinib and phenytoin.[14] Taken together with our results, we speculate that granulysin may be involved in the pathogenesis of early stage telaprevir-mediated dermatological adverse reactions possibly through induction of keratinocyte death.

Of five patients with grade 3 reactions, two patients without severe systemic manifestations did not have elevated serum granulysin of more than 10 ng/mL or did not have elevated levels before symptoms worsened. On the contrary, three patients with severe systemic manifestations had peak serum granulysin levels exceeding 10 ng/mL, and the symptoms of two patients with serum granulysin levels already exceeding 8 ng/mL at onset and within 6 days worsened. Therefore, serum granulysin tests may predict grade 3 dermatological adverse reaction with systemic manifestations. Furthermore, if serum granulysin levels elevate more than 8 ng/mL, more attention should be paid.

In Western countries, the prevalence of dermatological reactions in patients treated with telaprevir-based and

PEG IFN/RBV therapy are reported to be approximately 55% and 33%, respectively;[9,23] meanwhile, in Japanese patients, the respective rates are 74.9% and 58.7%. Moreover, approximately 4% and 9% of patients in Western and Japanese patients develop grade 3 reactions, respectively;[10] this is almost the same as that in the present study (10%). The difference may be due to genetic or ethnic variation. Therefore, genome-wide association studies may have identified a gene locus associated with telaprevir-induced severe dermatological reactions.

A limitation of this study is that the number of patients with grade 3 dermatological reactions is relatively small. However, the serum granulysin levels of patients with grade 3 dermatological reactions were significantly higher than those of other patients. Also, in two of the three patients with severe dermatological reactions, the serum granulysin level elevated before symptoms worsened, which are novel findings. Further study is required.

Triple therapy with the second-generation protease inhibitor simeprevir is reported to result in a similar prevalence of adverse reactions as PEG IFN and RBV combination therapy.[24,25] However, simeprevir is not approved worldwide. Although simeprevir-based triple therapy is effective, only 36–53% of prior non-responders achieve SVR.[24] Shimada *et al.* recently reported that by extending PEG IFN and RBV therapy from 24 to 48 weeks, telaprevir-based triple therapy improves the SVR to up to 68% in prior null responders.[26] Thus, telaprevir is a therapeutic option for prior null responders.

In conclusion, the present study suggests that male sex is a significant risk factor for severe telaprevir-induced dermatological reactions. In addition, serum granulysin levels are significantly associated with the severity of dermatological reactions and thus may be a good predictor of severe dermatological reactions with systemic manifestations in patients treated with telaprevir-based triple therapy.

ACKNOWLEDGMENTS

THIS STUDY WAS supported in part by grants from the Ministry of Education, Culture, Sports, Science and Technology of Japan, the Japan Society for the Promotion of Science, and the Ministry of Health, Labour and Welfare of Japan. The authors would like to thank all patients and their families as well as the investigators and staff of the 22 participating institutions. The principal investigators of the NORTE study sites are listed below in alphabetical order: Junichi Yoshida (Sapporo Social Insurance General Hospital), Atsushi Nagasaka (Sapporo City General Hospital), Akira Fuzinaga, Manabu Onodera (Abashiri-Kosei General Hospital), Hideaki Kikuchi, Tomofumi Atarashi (Obihiro-Kosei General Hospital), Ken Furuya (Hokkaido Social Insurance Hospital), Yukio Oohara, Sousi Kimura (National Hospital Organization Hokkaido Medical Center), Takuto Miyagihima (Kushiro Rosai Hosspital), Takashi Meguro (Hokkaido Gastroenterology Hospital), Akiyoshi Saga (Aiiku Hospital), Mineo Kudou (Sapporo Hokuyu Hospital), Jun Konno (Hakodate General Central Hospital), Kenichi Kumagaya (Hakodate Medical Association Hospital), Nobuaki Akakura (Sapporo Medical Center NTT EC), Tomoe Kobayashi (Tomakomai City Hospital), Uebayashi Minoru (Japanese Red Cross Kitami Hospital), Hiroshi Katou (Iwamizawa Municipal General Hospital), Yasuyuki Kunieda (Wakkanai City Hospital), Miki Tateyama (Tomakomai Nissho Hospital), Munenori Okamoto (Sapporo Century Hospital), Izumi Tunematsu (Touei Hospital) and Chuganji Yoshimichi (Tokyo Metropolitan Bokuto Hospital).

REFERENCES

1 Sakamoto N, Nakagawa M, Tanaka Y *et al.* Association of IL28B variants with response to pegylated-interferon alpha plus ribavirin combination therapy reveals intersubgenotypic differences between genotypes 2a and 2b. *J Med Virol* 2011; **83**: 871–8.
2 Poordad F, McCone J, Jr, Bacon BR *et al.* Boceprevir for untreated chronic HCV genotype 1 infection. *N Engl J Med* 2011; **364**: 1195–206.
3 Bacon BR, Gordon SC, Lawitz E *et al.* Boceprevir for previously treated chronic HCV genotype 1 infection. *N Engl J Med* 2011; **364**: 1207–17.
4 Zeuzem S, Andreone P, Pol S *et al.* Telaprevir for retreatment of HCV infection. *N Engl J Med* 2011; **364**: 2417–28.
5 Sherman KE, Flamm SL, Afdhal NH *et al.* Response-guided telaprevir combination treatment for hepatitis C virus infection. *N Engl J Med* 2011; **365**: 1014–24.
6 Jacobson IM, McHutchison JG, Dusheiko G *et al.* Telaprevir for previously untreated chronic hepatitis C virus infection. *N Engl J Med* 2011; **364**: 2405–16.
7 Kumada H, Toyota J, Okanoue T, Chayama K, Tsubouchi H, Hayashi N. Telaprevir with peginterferon and ribavirin for treatment-naive patients chronically infected with HCV of genotype 1 in Japan. *J Hepatol* 2012; **56**: 78–84.
8 McHutchison JG, Everson GT, Gordon SC *et al.* Telaprevir with peginterferon and ribavirin for chronic HCV genotype 1 infection. *N Engl J Med* 2009; **360**: 1827–38.
9 Roujeau JC, Mockenhaupt M, Tahan SR *et al.* Telaprevir-related dermatitis. *JAMA Dermatol* 2013; **149**: 152–8.

10 Torii H, Sueki H, Kumada H *et al.* Dermatological side-effects of telaprevir-based triple therapy for chronic hepatitis C in phase III trials in Japan. *J Dermatol* 2013; **40**: 587–95.
11 Chung WH, Hung SI, Yang JY *et al.* Granulysin is a key mediator for disseminated keratinocyte death in Stevens-Johnson syndrome and toxic epidermal necrolysis. *Nat Med* 2008; **14**: 1343–50.
12 Ogawa K, Takamori Y, Suzuki K *et al.* Granulysin in human serum as a marker of cell-mediated immunity. *Eur J Immunol* 2003; **33**: 1925–33.
13 Abe R, Yoshioka N, Murata J, Fujita Y, Shimizu H. Granulysin as a marker for early diagnosis of the Stevens-Johnson syndrome. *Ann Intern Med* 2009; **151**: 514–5.
14 Fujita Y, Yoshioka N, Abe R *et al.* Rapid immunochromatographic test for serum granulysin is useful for the prediction of Stevens-Johnson syndrome and toxic epidermal necrolysis. *J Am Acad Dermatol* 2011; **65**: 65–8.
15 Saigusa S, Ichikura T, Tsujimoto H *et al.* Serum granulysin level as a novel prognostic marker in patients with gastric carcinoma. *J Gastroenterol Hepatol* 2007; **22**: 1322–7.
16 Tanaka Y, Nishida N, Sugiyama M *et al.* Genome-wide association of IL28B with response to pegylated interferon-alpha and ribavirin therapy for chronic hepatitis C. *Nat Genet* 2009; **41**: 1105–9.
17 Aghemo A, De Francesco R. New horizons in hepatitis C antiviral therapy with direct-acting antivirals. *Hepatology* 2013; **58**: 428–38.
18 Lubbe J, Kerl K, Negro F, Saurat JH. Clinical and immunological features of hepatitis C treatment-associated dermatitis in 36 prospective cases. *Br J Dermatol* 2005; **153**: 1088–90.
19 Manns MP, McHutchison JG, Gordon SC *et al.* Peginterferon alfa-2b plus ribavirin compared with interferon alfa-2b plus ribavirin for initial treatment of chronic hepatitis C: a randomised trial. *Lancet* 2001; **358**: 958–65.
20 Yamada I, Suzuki F, Kamiya N *et al.* Safety, pharmacokinetics and resistant variants of telaprevir alone for 12 weeks in hepatitis C virus genotype 1b infection. *J Viral Hepat* 2012; **19**: e112–119.
21 Toyota J, Ozeki I, Karino Y *et al.* Virological response and safety of 24-week telaprevir alone in Japanese patients infected with hepatitis C virus subtype 1b. *J Viral Hepat* 2013; **20**: 167–73.
22 Bersoff-Matcha SJ, Miller WC, Aberg JA *et al.* Sex differences in nevirapine rash. *Clin Infect Dis* 2001; **32**: 124–9.
23 Cacoub P, Bourliere M, Lubbe J *et al.* Dermatological side effects of hepatitis C and its treatment: patient management in the era of direct-acting antivirals. *J Hepatol* 2012; **56**: 455–63.
24 Izumi N, Hayashi N, Kumada H *et al.* Once-daily simeprevir with peginterferon and ribavirin for treatment-experienced HCV genotype 1-infected patients in Japan: the CONCERTO-2 and CONCERTO-3 studies. *J Gastroenterol* 2014; **49**: 941–53.
25 Hayashi N, Seto C, Kato M, Komada Y, Goto S. Once-daily simeprevir (TMC435) with peginterferon/ribavirin for treatment-naive hepatitis C genotype 1-infected patients in Japan: the DRAGON study. *J Gastroenterol* 2014; **49**: 138–47.
26 Shimada N, Tsubota A, Atsukawa M *et al.* A 48-week telaprevir-based triple combination therapy improves sustained virological response rate in previous non-responders to peginterferon and ribavirin with genotype 1b chronic hepatitis C: a multicenter study. *Hepatol Res* 2014; [Epub ahead of print].

Abdominal Imaging

Abdom Imaging (2015)
DOI: 10.1007/s00261-015-0352-9

Intratumoral artery on contrast-enhanced computed tomography imaging: differentiating intrahepatic cholangiocarcinoma from poorly differentiated hepatocellular carcinoma

Seiji Tsunematsu,[1] Makoto Chuma,[1,5] Toshiya Kamiyama,[2] Noriyuki Miyamoto,[3] Satoshi Yabusaki,[3] Kanako Hatanaka,[4] Tomoko Mitsuhashi,[4] Hirofumi Kamachi,[2] Hideki Yokoo,[2] Tatsuhiko Kakisaka,[2] Yousuke Tsuruga,[2] Tatsuya Orimo,[2] Kenji Wakayama,[2] Jun Ito,[1] Fumiyuki Sato,[1] Katsumi Terashita,[1] Masato Nakai,[1] Yoko Tsukuda,[1] Takuya Sho,[1] Goki Suda,[1] Kenichi Morikawa,[1] Mitsuteru Natsuizaka,[1] Mitsuru Nakanishi,[1] Koji Ogawa,[1] Akinobu Taketomi,[2] Yoshihiro Matsuno,[4] Naoya Sakamoto[1]

[1]Department of Gastroenterology and Hepatology, Graduate School of Medicine, Hokkaido University, 15 Kita, 7 Nishi, Kita-ku, Sapporo 060-8638, Japan
[2]Department of Gastroenterological Surgery, Graduate School of Medicine, Hokkaido University, Sapporo, Japan
[3]Department of Diagnostic and Interventional Radiology, Graduate School of Medicine, Hokkaido University, Sapporo, Japan
[4]Department of Surgical Pathology, Hokkaido University Hospital, Sapporo, Japan
[5]Gastroenterological Center, Yokohama City University Medical Center, Yokohama, Kanagawa, Japan

Abstract

Aim: Differentiating intrahepatic cholangiocarcinoma (ICC) from poorly differentiated hepatocellular carcinoma (p-HCC) is often difficult, but it is important for providing appropriate treatments. The purpose of this study was to examine the features differentiating ICC from p-HCC on contrast-enhanced dynamic-computed tomography (CT).

Methods: This study examined 42 patients with pathologically confirmed ICC (n = 19) or p-HCC (n = 23) for which contrast-enhanced dynamic CT data were available. CT images were analyzed for enhancement patterns during the arterial phase, washout pattern, delayed enhancement, satellite nodules, capsular retraction, lesion shape, and presence of an intratumoral hepatic artery, intratumoral hepatic vein, intratumoral portal vein, and bile duct dilation around the tumor, portal vein tumor thrombus, lobar atrophy, or lymphadenopathy.

Results: Univariate analysis revealed the presence of rim enhancement (p = 0.037), lobulated shape (p = 0.004), intratumoral artery (p < 0.001), and bile duct dilation (p = 0.006) as parameters significantly favoring ICC, while a washout pattern significantly favored p-HCC (p < 0.001). Multivariate analysis revealed intratumoral artery as a significant, independent variable predictive of ICC (p = 0.037), and 15 ICCs (78.9%) showed this feature. Washout pattern was a significant, independent variable favoring p-HCC (p = 0.049), with 15 p-HCCs (65.2%) showing this feature.

Conclusion: The presence of an intratumoral artery in the arterial phase on contrast-enhanced dynamic CT was a predictable finding for ICC, and the presence of a washout pattern was a predictable finding for p-HCC, differentiating between ICC and p-HCC.

Key words: Intrahepatic cholangiocarcinoma—Intratumoral artery—Poorly differentiated hepatocellular carcinoma—Contrast-enhanced CT—Differential diagnosis

Correspondence to: Makoto Chuma; *email:* chuma@yokohama-cu.ac.jp

Published online: 13 January 2015

Intrahepatic cholangiocarcinoma (ICC) is the second most common primary liver malignancy after hepatocellular carcinoma (HCC) and originates from the epithelial lining of the intrahepatic bile duct [1]. Several studies have shown that the incidences of ICC and HCC have been increasing [2–4]. Contrast-enhanced dynamic-computed tomography (CT) has a primary role to play in the differential diagnosis of focal liver lesions, including HCC and ICC. Bile duct dilatation and rim-like contrast enhancement are frequently seen on contrast-enhanced CT of ICC [5]. Classic advanced HCC appears as a round tumor showing intense hyperenhancement in the arterial phase, followed by washout during dynamic imaging [6]. Knowledge of the typical imaging features of ICC and HCC would facilitate accurate diagnosis in most cases.

However, advanced HCCs such as poorly differentiated HCC (p-HCC) might not be as hypervascular as classic HCC, which might cause difficulty in differentiation from ICC. Differentiating ICC from p-HCC can reduce the risk of inappropriate treatments for ICC, such as transarterial chemoembolization aimed at HCC. ICC is usually fatal because of the lack of effective non-surgical therapeutic modalities, so correct diagnosis of ICC based on radiological findings may have prognostic significance, particularly in determining treatment methods [7]. Furthermore, definitive diagnosis of ICC will help oncologists to consider adequate treatments, such as complete resection including lymph node dissection.

Although some reports have described the radiological characteristics of ICC and HCC [5, 6, 8, 9], no reports appear to have described imaging findings for pathologically confirmed ICC and p-HCC. On contrast-enhanced CT, intratumoral arteries were often seen in ICC. However, there have been no previous reports that intratumoral arteries on CT distinguish ICC from HCC.

The purpose of this study was to assess the CT features and enhancement patterns differentiating ICC from p-HCC; furthermore, we evaluated whether the presence of an intratumoral artery could be an independent predictor for differentiating ICC from p-HCC.

Methods

Patients

This study was approved by the ethics committees of Hokkaido University Hospital. All study protocols were approved by the institutional review board and performed in compliance with the Declaration of Helsinki.

We retrospectively searched the surgical treatment database at our hospital from July 2003 to December 2012, using the search terms "poorly differentiated HCC" and "ICC." Forty-two patients with histopathological confirmation of either ICC (n = 19) or p-HCC (n = 23) who had undergone contrast-enhanced CT in our institution were included in this study. The final diagnosis of all tumors was confirmed by histopathological examination of surgical specimens. Histological diagnosis was made according to World Health Organization criteria [10, 11]. Combined-type liver cancers were excluded to more clearly investigate differential points of CT imaging between poorly differentiated HCC and ICC. Patient demographics and tumor characteristics are summarized in Table 1.

The 19 patients with ICC included 13 men and 6 women (age range 48–79 years), while the 23 patients with p-HCC included 19 men and 4 women (age range 37–79 years). Serum levels of hepatitis B surface antigen and hepatitis C antibody, alpha-fetoprotein (AFP), protein induced by vitamin K absence or antagonist-II (PIVKA-II), carcinoembryonic antigen (CEA), and carbohydrate antigen 19-9 (CA19-9) were examined preoperatively in all patients.

Image analysis

CT images were obtained by using Aquilion 64 (n = 16, Toshiba Medical Systems, Tochigi, Japan), Aquilion 4-slice CT (n = 12, Toshiba Medical Systems, Tochigi, Japan), light Speed VCT (n = 6, GE, Waukesha, WI, USA), Somatom Volume Zoom (n = 4, Siemens Medical Solutions, Erlangen, Germany), and Somatom Sensation 64 (n = 4, Siemens AG Medical Solutions, Erlangen, Germany).

Unenhanced and 3-phase contrast-enhanced helical CT images were obtained. An automatic bolus-tracking program (Real Prep; Toshiba Medical Systems) was used to time the start of scanning for each phase after contrast material injection. Monitoring was performed at the level of the L1 vertebral body, with the region of interest cursor (0.8–2.0 cm^2) placed in the abdominal aorta. Real-time serial monitoring studies began 10 s after the start of contrast injection. The trigger threshold level was set at 200 Hounsfield units. Arterial phase and portal venous phase scanning started at 20 and 40 s after triggering, respectively. Delayed phase scanning started 180 s after the contrast injection. Contrast material (mean, 450 mg of iodine per kilogram body weight) was delivered over a period of 30 s.

Two radiologists (N.M. and S.Y. with 18 and 8 years of post-training experience in interpreting body CT images, respectively) who had no knowledge of clinical patient information performed all measurements by using a commercially available Digital Imaging and Communications in Medical viewer (VOX BASE; J-MAC, Sapporo, Japan).

The following CT features were evaluated: (1) lesion size; (2) satellite nodules (Fig. 1A); (3) capsular retraction (Fig. 1B); (4) lobulated shape of lesion (Fig. 1C); (5) rim enhancement during arterial phases (Fig. 1C); (6) intrahepatic bile duct dilation around the tumor

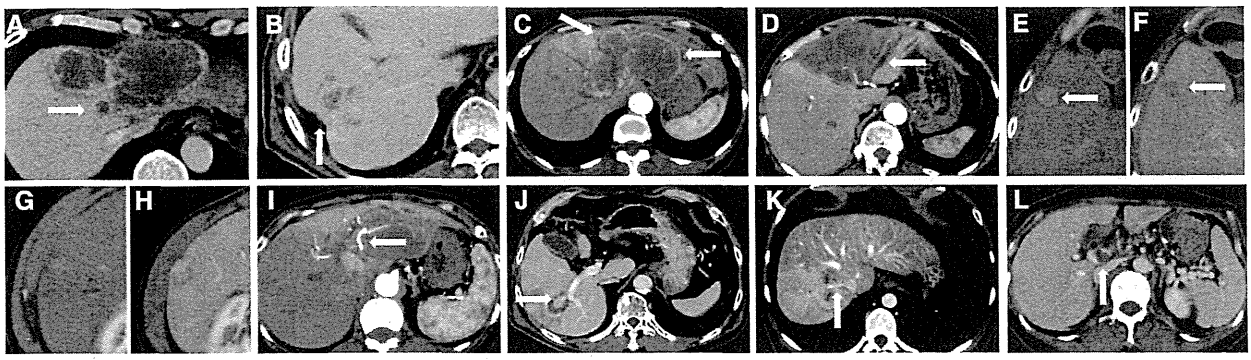

Fig. 1. Evaluated imaging features of contrast-enhanced CT for tumors. **A** CT during the arterial phase with p-HCC shows the satellite nodule (*arrows*). **B** CT during the delayed phase with ICC shows capsular retraction (*arrow*). **C, D** CT during the arterial phase with ICC shows a lobulated lesion and rim enhancement (*arrows*) (**C**) and intrahepatic bile duct dilation around the tumor (*arrow*) (**D**). **E, F** CT during the arterial phase (**E**) and delayed phase (**F**) with p-HCC shows arterial enhancement (**E**) and a washout pattern. **G, H** CT during the arterial phase (**G**) and delayed phase (**H**) with p-HCC shows delayed enhancement. **I–K** CT with ICC shows a hepatic artery running into the tumor (*arrow*) (**I**, arterial phase), a branch of the portal vein running into the tumor (*arrow*) (**J**, portal venous phase), and a hepatic vein running into the tumor (*arrow*) (**K**, delayed phase). **L** CT during the portal venous phase with p-HCC shows tumor thrombus in the portal vein (*arrow*).

Table 1. Patient characteristics of intrahepatic cholangiocarcinoma or poorly differentiated hepatocellular carcinoma

	ICC (n = 19)	p-HCC (*n* = 23)	*p* value
Gender (male/female)	13/6	19/4	0.283
Age (years)	63 (48–79)	62 (37–79)	0.535
Chronic viral hepatitis (HBV/HCV)	3 (2/1)	20 (11/9)	<0.001
Albumin (g/dL)	4.0 (3.1–4.6)	4.0 (3.1–5.2)	0.836
Total bilirubin (mg/dL)	0.8 (0.4–1.4)	0.9 (0.4–2.3)	0.389
Prothrombin time (%)	97 (79.3–135)	87 (66.1–111)	0.038
Platelet ($\times 10^4/\mu L$)	233 (122–354)	135 (42.0–305)	<0.001
AFP (10 ng/mL)	5.8 (2.3–80)	1360 (4.30–39,500)	<0.001
PIVKA-II (40 mAU/mL)	24 (7.0–1400)	208 (9.0–245,600)	0.002
CEA (5 ng/mL)	4.8 (1.0–345)	3.1 (1.4–9.1)	0.287
CA19-9 (37 U/mL)	45.1 (1.0–2590)	47.4 (1.0–237)	0.751

HBV hepatitis B virus, *HCV* hepatitis C virus, *AFP* alpha-fetoprotein, *PIVKA-II* protein induced by vitamin K absence or antagonist-II, *CEA* carcinoembryonic antigen, *CA19-9* cancer-associated carbohydrate antigen 19-9

(Fig. 1D); (7) arterial enhancement (Fig. 1E); (8) washout pattern (Fig. 1E, F); (9) delayed enhancement (Fig. 1G, H); (10) intratumoral artery during arterial phases (Fig. 1I); (11) intratumoral portal vein (Fig. 1J); (12) intratumoral hepatic vein (Fig. 1k) and portal vein tumor thrombus (Fig. 1L); (13) lobar atrophy; and (14) lymphadenopathy. The washout pattern was defined as arterial enhancement (due to the presence of non-triadal neo-angiogenetic arteries) and portal/venous wash out (due to the loss of sinusoidal vascularization) on dynamic imaging.

Particularly, an intratumoral artery was defined as an artery entering the tumor and remaining inside the tumor. Intratumoral portal veins and intratumoral hepatic veins were defined in a similar way. Although minimal discrepancies were seen between readers when interpreting the shape of lesions, consensus decisions for these discrepancies were easily reached during an additional reading session.

Statistical analysis

We statistically analyzed differences in clinical characteristics and CT imaging features between ICC and p-HCC by using the Chi square test for categorical variables and the non-parametric Mann–Whitney *U* test for continuous variables. Significant variables obtained from univariate analysis were applied to multivariate stepwise binary logistic regression analysis to determine the optimal findings for differentiating ICC from p-HCC. Statistical analyses were performed by using the SPSS software package, version 20.0 (IBM, NY). For all tests, values of $p < 0.05$ were considered statistically significant.

Results

Characteristics of patients with ICC or p-HCC

Baseline characteristics of patients with ICC or p-HCC are summarized in Table 1. There were no significant

Table 2. Uni- and multivariate analysis of contrast-enhanced CT features of intrahepatic cholangiocarcinoma and poorly differentiated hepatocellular carcinoma

Pattern	ICC (n = 19)	p-HCC (n = 23)	Univariate analysis p	Multivariate analysis	
				p	Odds ratio (95% CI)
Mean diameter (mm)	64.4 (25–150)	53.7 (10–150)	0.192		
Lobulated shape	14 (73.7)	9 (39.1)	0.004	0.550	1.951 (0.218–17.445)
Satellite nodule	15 (78.9)	14 (60.1)	0.207		
Capsular retraction	6 (31.6)	5 (21.7)	0.407		
Arterial enhancement	9 (47.3)	17 (73.9)	0.078		
Bile duct dilatation	11 (57.9)	4 (17.4)	0.006	0.323	3.445 (0.296–40.070)
Rim enhancement	13 (48.4)	4 (17.4)	0.037	0.158	6.068 (0.495–74.308)
Delayed enhancement	8 (42.1)	7 (30.4)	0.432		
Washout	1 (5.3)	15 (65.2)	<0.001	0.049	0.087 (0.008–0.993)
Intratumoral artery	15 (78.9)	8 (34.8)	<0.001	0.037	10.192 (1.155–89.954)
Intratumoral portal vein	7 (36.8)	2 (8.7)	0.055		
Intratumoral vein	3 (15.8)	2 (8.7)	0.581		
Portal vein tumor thrombus	1 (5.3)	4 (17.4)	0.197		
Lobar atrophy	6 (31.6)	2 (8.7)	0.060		
Lymphadenopathy	4 (21.1)	1 (4.3)	0.094		

Values in parentheses represent percentages

differences between the 2 groups with regard to sex, age, albumin, total bilirubin, CEA, and CA19-9. However, there were differences with respect to chronic viral hepatitis, prothrombin time, platelet counts, AFP, and PIVKA-II.

Analyses of contrast-enhanced CT features of ICC and p-HCC

CT features of ICC and p-HCC and the results of univariate analysis are summarized in Table 2. Lesion diameter ranged from 2.5 to 15.0 cm (mean 64.4 mm) for ICC and from 1.0 to 15.0 cm (mean 53.7 mm) for p-HCC (p = 0.192). Lobulated lesion shape was significantly more rare in patients with p-HCC (n = 9, 39.1%) than in patients with ICC (n = 14, 73.7%) (p = 0.004). The presence of satellite nodules was not statistically significantly different between ICC (n = 15, 78.9%) and p-HCC (n = 14, 60.1%) (p = 0.207). Significant differences in arterial enhancement were not seen between ICC (n = 9, 47.3%) and p-HCC (n = 17, 73.9) (p = 0.078). Capsular retraction was present in patients with ICC (n = 6, 31.6%) or p-HCC (n = 5, 21.7%) (p = 0.407). The presence of intrahepatic bile duct dilation around the tumor differed significantly between the ICC group (n = 11, 57.9%) and the p-HCC group (n = 4, 17.4%) (p = 0.006). Peripheral rim enhancement in the arterial phase was less common in the p-HCC group (n = 4, 17.4%) than in the ICC group (n = 13, 48.4%) (p = 0.037). A washout pattern was more frequent in p-HCC (n = 15, 65.2%) than ICC (n = 1, 5.3%) (p < 0.001). There was no significant difference (p = 0.432) in the occurrence of delayed enhancement in p-HCC (n = 8, 42.1%) and in ICC (n = 7, 30.4%).

An intratumoral artery in the arterial phase was more frequently present for ICC lesions (n = 15, 78.9%) than p-HCC (n = 8, 34.8%) (p < 0.001). The ICC group more frequently showed an intratumoral portal vein (n = 7, 36.8%) than the p-HCC group (n = 2, 8.7%) (p = 0.055). An intratumoral hepatic vein was rarely exhibited in ICCs (n = 3, 15.8%) or p-HCCs (n = 2, 8.7%) (p = 0.581). Portal vein tumor thrombus was also rarely present in ICCs (n = 1, 5.3%) or p-HCCs (n = 4, 17.4%) (p = 0.197).

There was no significant difference (p = 0.060) in the presence of lobar atrophy in ICC (n = 6, 31.6%) and in p-HCC (n = 2, 8.7%). Lymphadenopathy was present in patients with ICC (n = 4, 21.1%) or p-HCC (n = 1, 4.3%) (p = 0.407).

Next, we conducted multivariate binary logistic regression analysis by using significant parameters from the univariate analysis. As shown in Table 2, the presence of an intratumoral artery was an independent CT predictor for differentiating ICC from p-HCC (p = 0.037, odds ratio = 10.192); on the contrary, washout pattern was a significant parameter favoring p-HCC (p = 0.049, odds ratio = 0.087). The presence of an intratumoral artery on CT had a sensitivity of 78.9% and a specificity of 65.2% for ICC. Furthermore, the presence of an intratumoral artery on CT had a positive predictive value of 65.2% and a negative predictive value of 78.9% for ICC.

Case presentation

Representative images from CT and histological features in patients with ICC and p-HCC are shown in Figs. 2 and 3. A 60-year-old man (Case 1) presented with a massive, advanced tumor predominantly located in the right lobe of the liver, and a hepatic artery was seen running into the tumor on CT (Fig. 2A). A right hepatic lobectomy was performed, and histological examination revealed ICC tumor cells that showed infiltrating

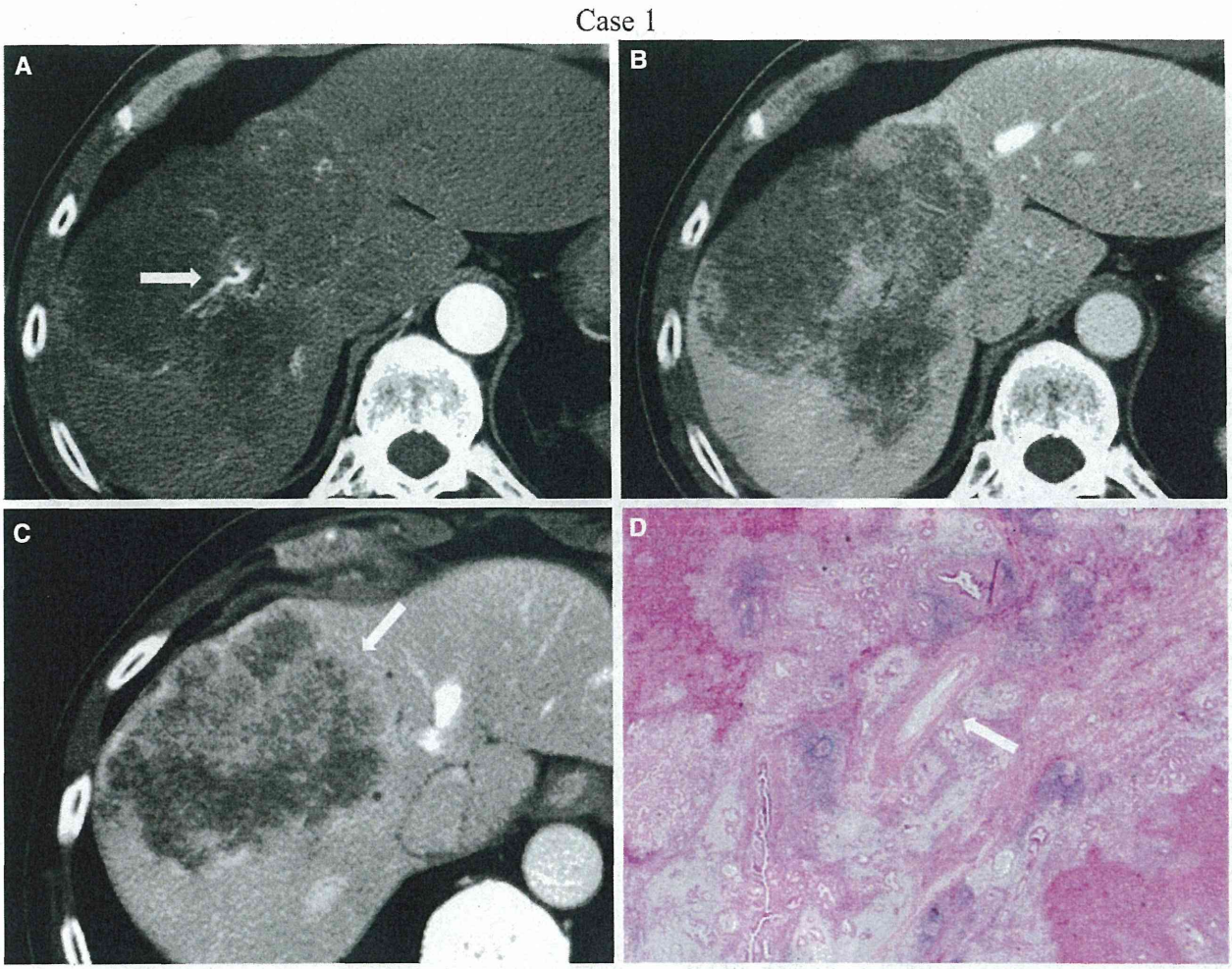

Fig. 2. Contrast-enhanced CT and histological features of ICC. **A** ICC in a 60-year-old man shows a subtle intratumoral artery on arterial phase CT (*arrow*). **B**, **C** CT on delayed phase shows the absence of delayed enhancement (**B**) and the presence of a lobulated shape (**C**). **D** ICC tumor cells show infiltrating replacement growth of the surrounding hepatic parenchyma. An intratumoral artery that has not been destroyed by tumor cells is identified (*arrow*). (Original magnification: d × 10. Hematoxylin and eosin staining).

replacement growth against the surrounding hepatic parenchyma. An intratumoral artery that had not been destroyed by tumor cells was identified (Fig. 2D). A 58-year-old woman (Case 2) presented with a massive, advanced tumor predominantly located in the left lobe of the liver, and no intratumoral artery, portal vein, or hepatic vein was identified on CT (Fig. 3A). A left hepatic lobectomy was performed, and histological examination revealed p-HCC. The tumor was compressing the surrounding liver, and compressed vessels were clearly visible (Fig. 3D).

Discussion

On contrast-enhanced CT, the typical appearance of ICC is a mass that demonstrates thin, rim-like, or thick, band-like contrast enhancement around the tumor during arterial and portal venous phases, with satellite nodules, capsular retraction, lobar atrophy, lymphadenopathy, and delayed enhancement [12–15]. The accuracy of contrast-enhanced CT in diagnosing ICC was 70% [16]. The finding of satellite nodules was associated with tendency to invade small portal vessels and along portal triads. Additionally, scirrhous stroma and biliary involvement of ICC have an influence on the imaging of capsular retraction and lobar atrophy. In our study, a lobulated shape was more closely associated with ICC than with p-HCC on univariate analysis, although satellite nodules, capsular retraction, lobar atrophy, and lymphadenopathy were not different between ICC and p-ICC. The finding of lobulated shape supported the results of previous studies [17, 18]. This trend may be

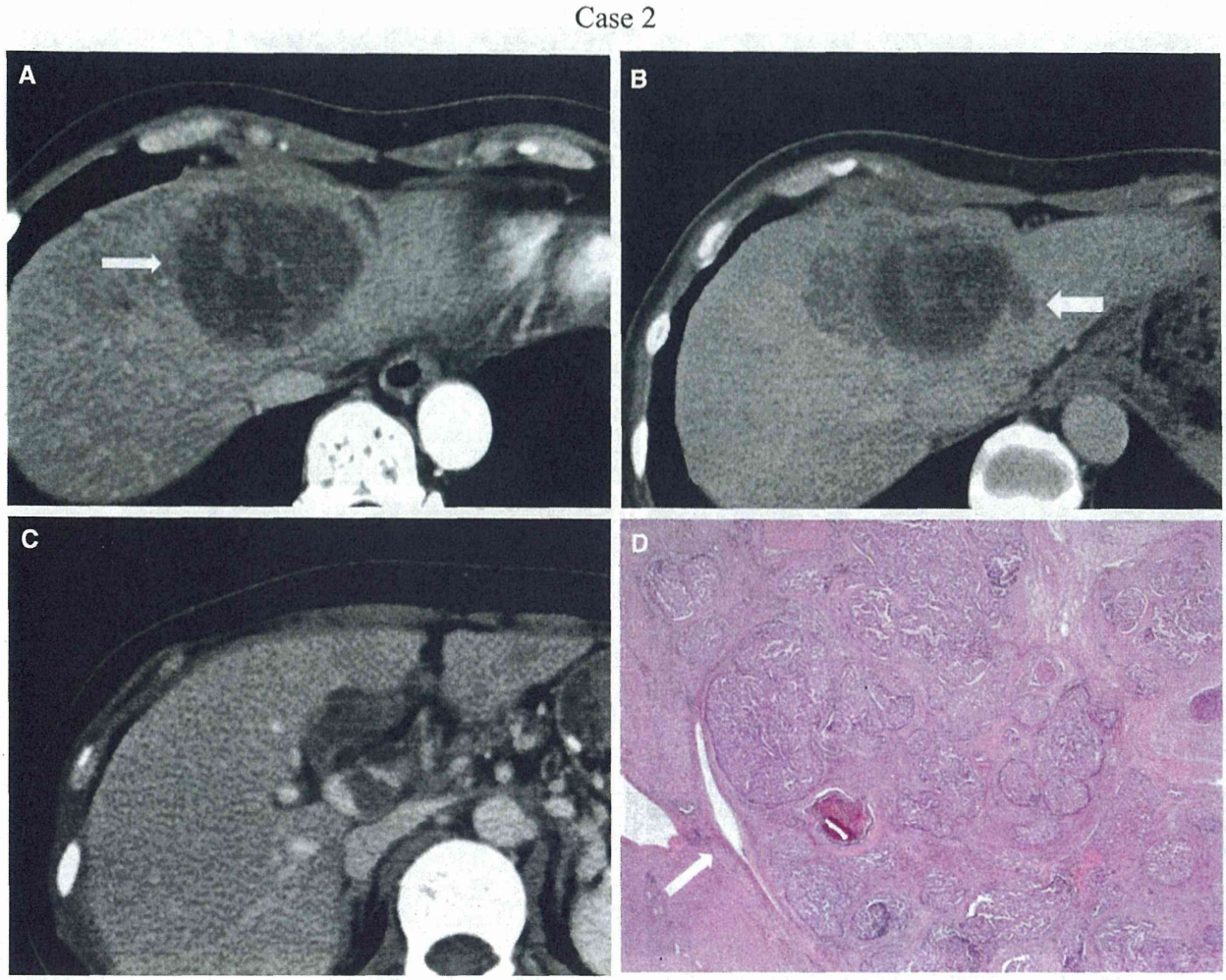

Fig. 3. Contrast-enhanced CT and histological features of p-HCC. **A** p-HCC in a 58-year-old woman shows a low attenuating tumor on arterial phase CT (*arrow*). **B** CT on delayed phase shows nodule (*arrow*) and the absence of delayed enhancement. **C** CT on portal venous phase shows portal vein tumor thrombus. **D** Compressive growth of p-HCC. Tumor compresses the surrounding liver and compressed vessels are clearly visible (*arrow*). (Original magnification: d × 10. Hematoxylin and eosin staining).

related to the fact that ICC tends to invade small portal vein branches adjacent to the main tumor, and the fusion of the primary mass and adjacent satellite tumors results in the lobulated shape [19]. Tumor shape could thus represent a differential feature between ICC and p-HCC.

The frequency of intrahepatic bile duct dilation around the tumor differed between ICC and p-HCC. Eleven of the 19 ICC tumors were accompanied by intrahepatic bile duct dilation around the tumor. The presence of intrahepatic bile duct dilation around the tumor may thus provide a useful clue for differentiation.

In our study, 13 ICC showed rim enhancement during the arterial phase. Rim enhancement patterns differing from p-HCC may relate to different pathological components in the tumor [20]. Fan et al. suggested that the degree of enhancement of ICC depends on the proportion of component fibers and tumor cells, with a tumor rich in cells resulting in strong enhancement [9]. ICC that is peripherally rich in tumor cells with fibrosis in the central portion may result in peripheral rim-like hyperenhancement.

In addition, significant differences in washout patterns were seen between ICC and p-HCC, although there were no significant differences in arterial enhancement and delayed enhancement between the two groups. According to the guidelines of the American Association for the Study of Liver Disease, nodules larger than 1 cm detected in liver cirrhosis may be confidently diagnosed as HCC only when a washout pattern is detected on contrast-enhanced CT or magnetic resonance imaging